Crystal Growth: Physics, Technology and Modeling

Stanisław Krukowski & Michał Leszczyński
Institute of High Pressure Physics PAS
01-142 Warsaw, Sokołowska 29/37
e-mail: stach@unipress.waw.pl, mike@unipress.waw.pl

Sławomir Kret
Institute of Physics PAS
02-668 Warsaw, Al. Lotników 32/46
E-mail: kret@ifpan.edu.pl

Lecture 10. Selected methods of transmission electron microscopy
26 April 2022

http://w3.unipress.waw.pl/~stach/cg-2021-22/

First experimental TEM

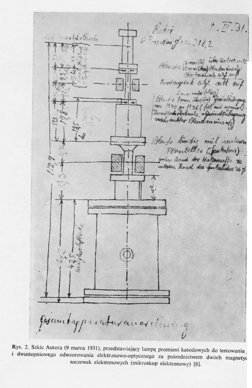

Rys. 2. Szkic Autora (9 marca 1931), przedstawiający lampę promieni katodowych do testowania i dwustopniowego odwzorowania elektronowo-optycznego za pośrednictwem dwóch magnety soczewek elektronowych (mikroskop elektronowy) [8].

Ernst Ruska **and** ***Max Knoll*** **built the first electron microscope in 1931**
(Nobel Prize to Ruska in 1986)

Transmission Electron Microscopy

Direct information from inside of material on :

- type and density of defects
- elemental and phase composition
- strain field distribution (3D)
- local electric and magnetic fields (up to 1 nm)
- interfaces atomic structure
- crystalography

- resolution depending on the operating mode but belów 35 pm is possible in same cases

- Thin sample
- Local info
- Destructive

Convectional TEM like biological light microscope

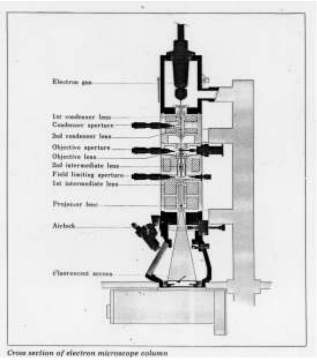

Cross section of electron microscope column

Jeol 2000EX IFAPN from 1989
200KV 0.27 nm Lab6 catode

The Genesis of TEM

In 1923, Prince Louis de Broglie postulated the wave nature of matter.

In 1927, Hans Bush showed that magnetic coils can focus an electron beam in the same way as glass lenses to light.

In 1927 C.J. Davisson and L.H Germer and G. P. Thompson and A. Reid independently demonstrated electron diffraction => the wave nature of electrons confirmed.

On April 7, 1931, Ernst Ruska and Max Knoll obtained the first TEM image using two magnetic lenses.

1936 - the first commercial TEM- Metropolitan-Vickers EM1.

Modern aberation corrected TEM/STEM

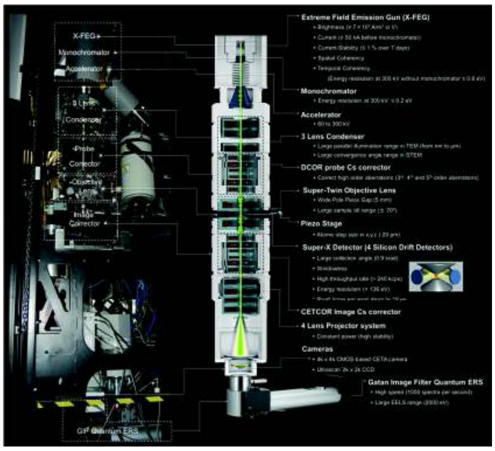

Cryo-electron microscopy innovators win 2017 Nobel Prize in Chemistry for developing cryo-electron microscopy for the high-resolution structure determination of biomolecules in solution
Direct electron detection technology

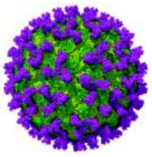

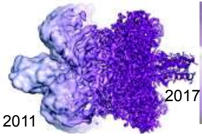

2011

2017

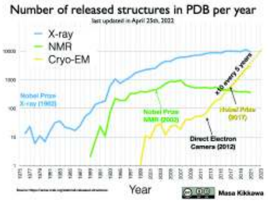

But we will not
talk about …..

Circular aperture Diffraction of fotons or electrons- Difraction limit

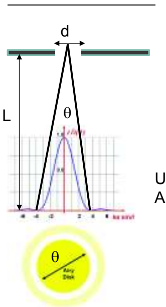

Airy Disk
These rings are produced by Fraunhofer Diffraction by the circular aperture.
L>>λ

Using the small angle approximation
Airy dysk diameter θ in radians

$$d\ sin\theta = 1.22\lambda \qquad \theta \cong 1.22\frac{\lambda}{d}$$

---

50 YEARS OF Electron Microscopy Group (EMG) of Institute of Physics Polish Academy of Sciences

IFPAN from September 2010 TITAN^3 CUBED 80-300 KV
Resolution in TEM → 0.07 nm Energy resolution EELS →0.2eV
Electron Holography, EDX, STEM, HADAF , Lorentz

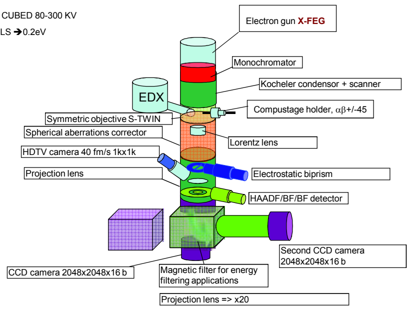

According to the Rayleigh Criterion, two point sources cannot be resolved if their separation is less than the radius of the Airy disk. The Airy disk is named for the English astronomer Sir George Biddell Airy, who served as the seventh Astronomer Royal from 1835-1881

Abbe Resolution = 2λ/NA2 1873

$$d_0 = \frac{\lambda}{NA} = \frac{\lambda}{2n\sin\theta}$$

refined by Lord Rayleigh in 1896

$$d_0 = \frac{0.61\lambda}{\mathrm{n}\sin\theta} \approx \frac{0.61\lambda}{\sin\theta}$$

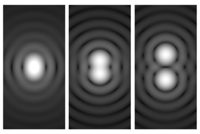

For electrons n=1, and small angles

So for better resolution θ↑ and λ↓

Young's double-slit experiment performed with electrons .

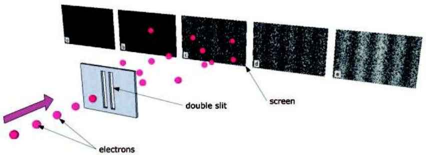

Image by Mehul Malik

3D crystal

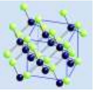

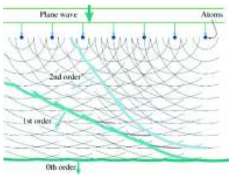

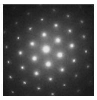

Electron dyfractogram

A plane, coherent electron wave generates secondary wavelets from a row of scattering centers (atoms)
The secondary wavelets interfere, resulting in a strong direct (zeroorder) beam and several (higher order) beams scattered (diffracted) at specific angles.

---

wavelength of electrons

L. De Broglie 1924
Phil. Mag.,47 446
λ=h/p =h/mv

h Planc constant
p the momentum of the particle

$$\lambda_B = \frac{h}{mv} = \frac{h}{\frac{m_0}{\sqrt{1-\frac{v^2}{c^2}}}v} = \frac{h\sqrt{1-\frac{v^2}{c^2}}}{m_0 v}$$

Accelartaion voltage	λ [nm]	λ (nm) relatywistic	% of c
100	0.00386	0.00370	0.54%
200	0.00273	0.00251	0.69%
300	0.00223	0.00197	0.77%

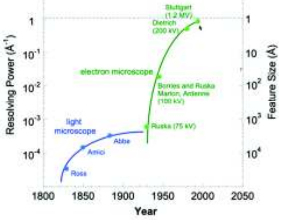

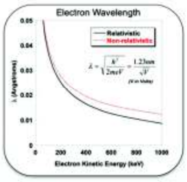

Resolution limit due to spherical aberation

C_3 spherical aberration coefficient of objective lens

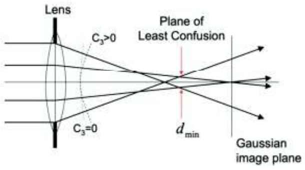

For a lens with aperture angle α, the minimum blur is $d_{\min} = \frac{1}{2} C_3 \alpha^3$

Typical TEM numbers: C_3= 1 mm, α=10 mrad → d_{min}= 0.5 nm

The interaction of high-energy electrons with an atom - energy 30-1000 KeV

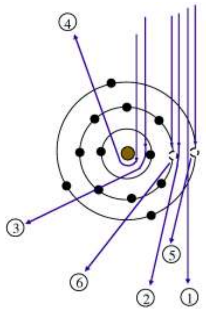

1. Not scattered electron
2. Low angle elastic scattering
3. High angle elastic scattering
4. Backward scatter
5. Inelastic scattering on outer shell
6. Inelastic scattering on inner shell

Resolution limit due to spherical aberation minimum bem spot in STEM

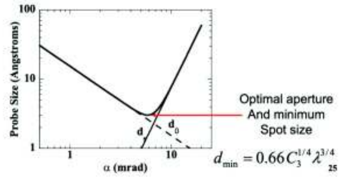

$d_{\min} = 0.66 C_3^{1/4} \lambda^{3/4}$ 25

For a rough estimate of the optimum aperture size, convolve blurring terms

-If the point spreads were gaussian, we could add in quadrature:

$$d_{tot}^2 \approx d_0^2 + d_s^2 = \left(\frac{0.61\lambda}{\alpha_0}\right)^2 + \left(\frac{1}{2} C_3 \alpha_0^3\right)^2$$

The interaction of high-energy electrons with a solid - inelastic scattering

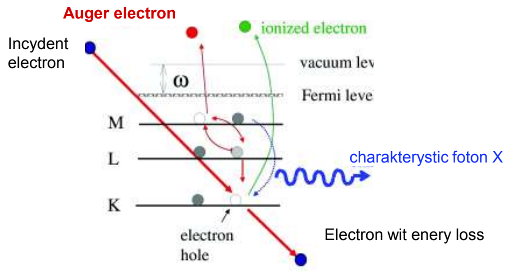

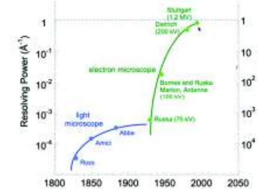

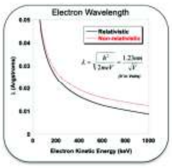

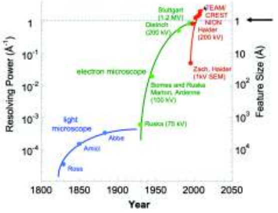

Aberration correction technology
Sub angstrom microscopy
Resolution in pm

Aberration correctors are complex
and computers are needed
to optimize construction
and for working

After David A. Muller , Nature Materials 2009, https://www.paradim.org/2021_CU_SS

The signals produced by an electron probe in a thin crystal used for imaging and / or spectroscopy

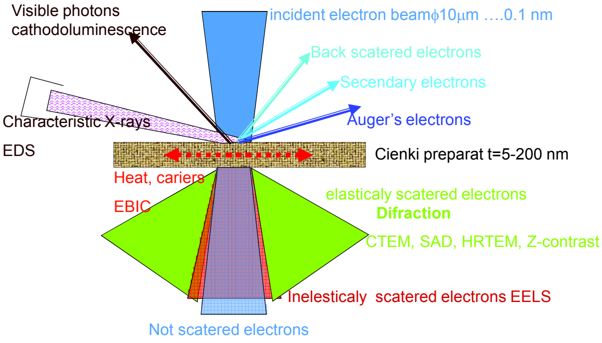

Why are electrons so interesting?

	Scattered on :	Mean free path [nm]	Absorption lenght [nm]
Neutrons	nucleus	10^7	10^8
X-rays	electrons	10^3	10^5
electrons	potential	10	10^2

Very strong interaction with matter

The signal from 1 atom in the sample for electrons is 10^4 biger then for X-rays !!

IFPAN from Jun 2010

Electron resolution

- ➔ 0.9 nm @ 15 kV
- ➔1.4 nm @ 1 kV

Ion resolution

- ➔ 5.0 nm @ 30kV

Ion energy 500V-30kV

EDX

Omiprobe

GIS- Pt

GIS-W

Thin electron transparent sample : 10-50 nm grubości

- Ion milling

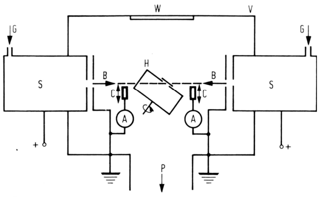

Schematic drawing of an ion etching apparatus

V — Vacuum chamber,
W — Viewing window,
P — Vacuum pump,
B — Ion beam,
S — Ion sources,
G — Gas inlet,
C — Ion current collector,
A — Ammeter,
H — Rotating specimen holder

Image from:Electron Microscopy in Solid Stage Physics H.Bethge and J. Heydenreich , Elesevier 1987

Ion beam incidence angle 1-25 ° but <5 ° avoids selective etching

Accelerating voltage 4-9kV (200V- 8kV) time 1-48h

Argon ions, cooling with liquid nitrogen indirectly, (with a stream of inert gas)

vacuum 10-5 Torr (10-3 Torr when etching)

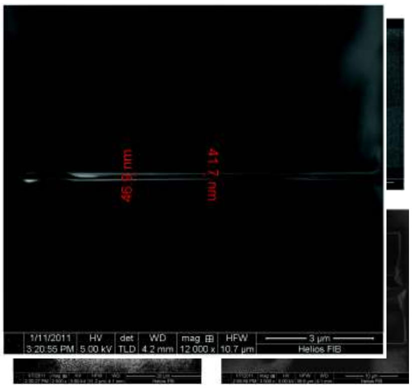

Photo B.Kurowska
M.Klepka

Ion milling => Radiation damage , surface amorphization

Damage limitation by: lower voltage, reducing the angle of incidence of the ion beam, cooling of sample

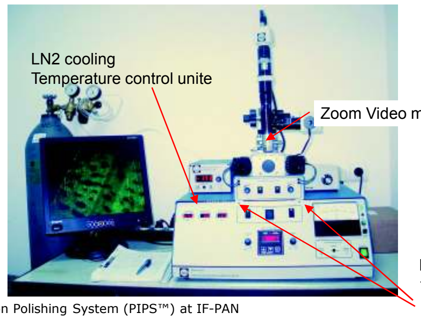

LN2 cooling
Temperature control unite

Zoom Video mikroskope

Ion guns
100V - 6KV
angles 0º-10º

Precision Ion Polishing System (PIPS™) at IF-PAN

Basic Modes of Operation of the TEM microscope

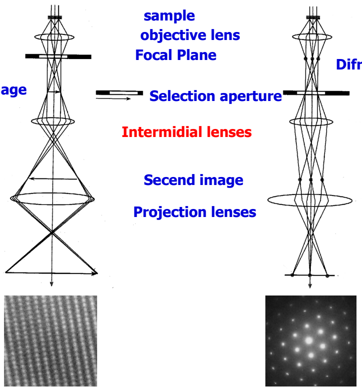

sample
objective lens
Focal Plane
Contrast aperture
Difraction plane
First image
Selection aperture
Intermidial lenses
Secend image
Projection lenses
HRTEM
Electron diffraction

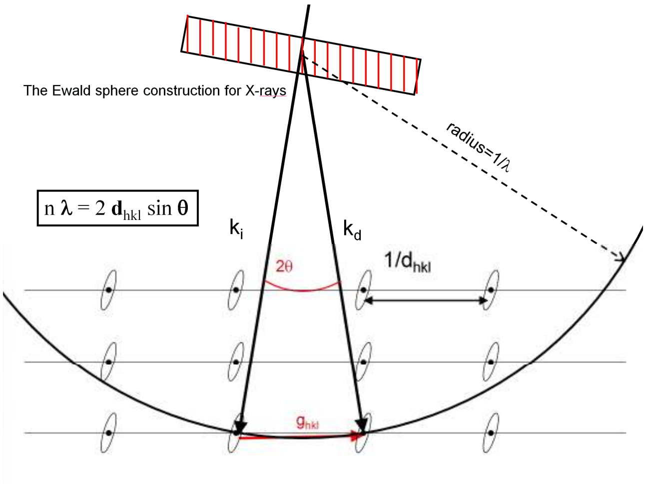

The Ewald sphere construction for X-rays

$$\boxed{n\,\lambda = 2\,\mathbf{d}_{hkl}\,\sin\theta}$$

Diffraction contrast: bright and dark field

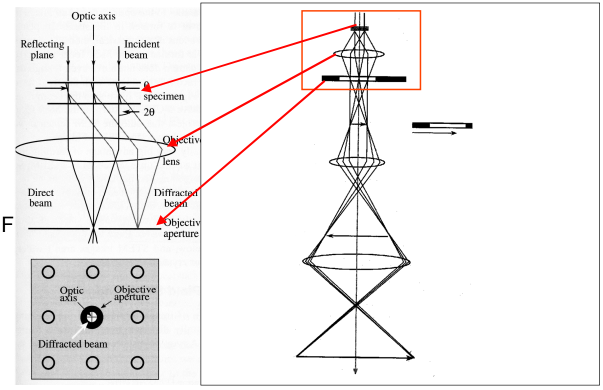

BF

Rys:. D. Williams et.al., "Transmission Electron Microscopy. A textbook for Materials Science", .

The Ewald sphere for high energy electrons

Diffraction occurs when the Ewald sphere intersects a reciprocal lattice nodes

For 200 kV electrons,
1/λ = 1/0.00273 nm = 366 nm-1

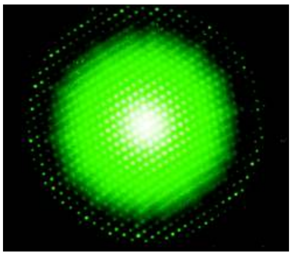

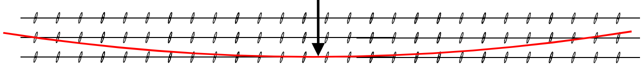

Two-beam conditions for Si near 001 zone axis

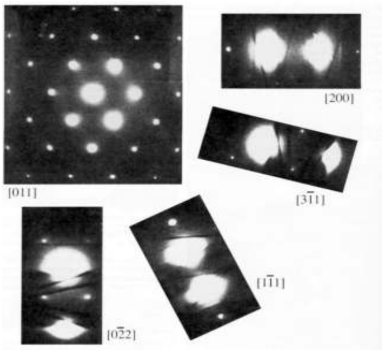

Picures from : D. Williams et.al., "Transmission Electron Microscopy. A textbook for Materials Science", .

Electron difraction

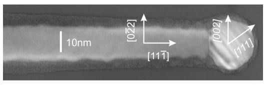

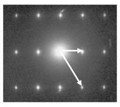

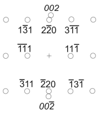

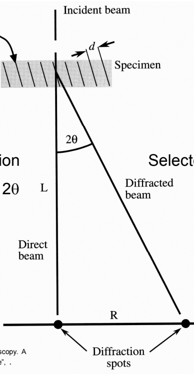

Bragg equation

λ/d=2 sin θ ≅ 2θ

So:

$$\boxed{R = L\lambda/d}$$

Selected area difraction SAD from ZnTe nanowire

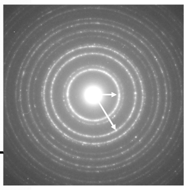

Difraction from mamy nanowires as X-ray powder difraction

Ryssunek : D. Williamset.al., "Transmission Electron Microscopy. A textbook for Materials Science", .

Fot. P.Dluzewski, S.Kret IF-PAN

Diffraction contrast: bright and dark field
Pd crystallites 5-15 nm

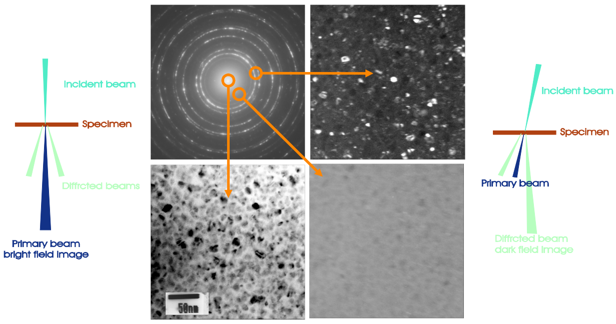

Foto :P.Dłużweski IF-PAN

PERFECT CRYSTALS ➔ Thickness contours depend also of material

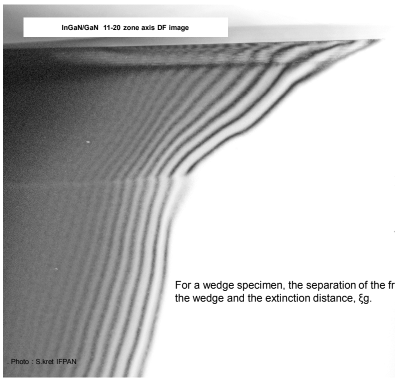

. Photo : S.kret IFPAN

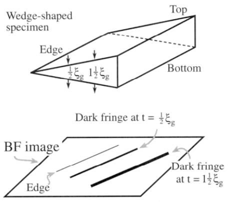

For a wedge specimen, the separation of the fringes in the image is determined by the angle of the wedge and the extinction distance, ξg.

HRTEM image formation

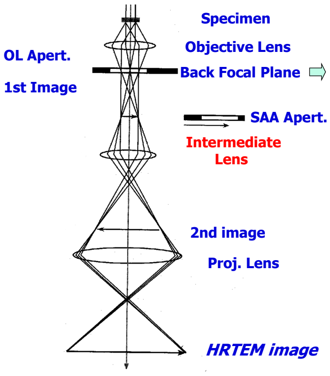
Specimen

OL Apert.

Objective Lens

Back Focal Plane ⇨

1st Image

SAA Apert.

Intermediate Lens

2nd image

Proj. Lens

HRTEM image

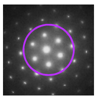

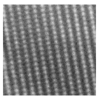

Diffraction contrast: bright and dark field

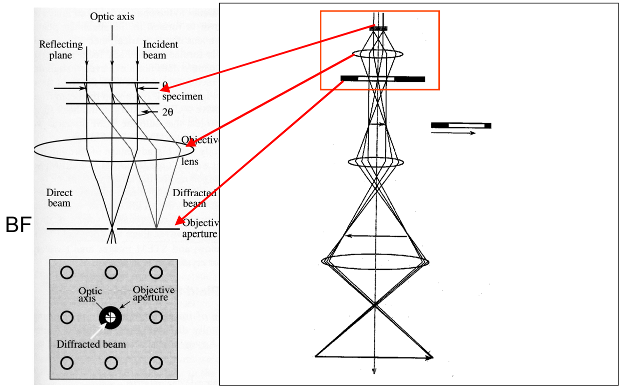

Rys:. D. Williams et.al., "Transmission Electron Microscopy. A textbook for Materials Science", .

HRTEM image formation

beams selection of on the diffraction pattern

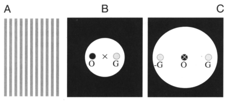

2 beams interference

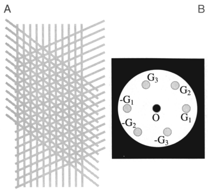

7 beams interference

Images from D. Williamset.al., "Transmission Electron Microscopy. A textbook for Materials Science", .

CRYSTAL WITH DEFECTS

Intuitive description of diffraction contrast of dislocation

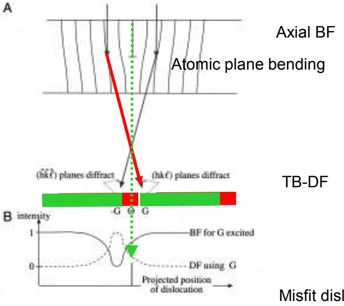

Axial BF

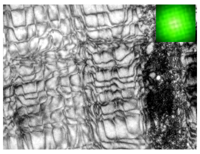

TB-DF

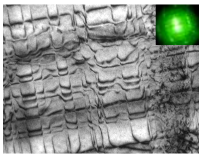

Photo :P.Dłużewski IF-PAN
Sample Ł. **GELCZUK** et.al. WEMiF ,Wrocław

Misfit dislocations GaAs/$In_{0.07}Ga_{0.93}As$

HRTEM GaAs <110>

Don't forget about aberration of the lenses and MTF of the microscope
➔ You can put smaller diaphragm to minimize the aberrations

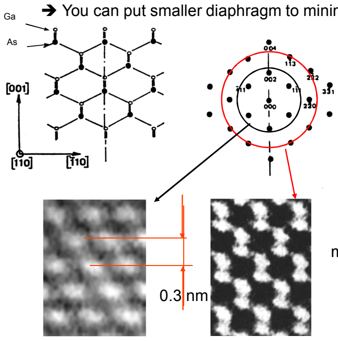

monolayer

7 beams

Resolution:

0.27 nm

13 beams
Resolution 0.16 nm

HRTEM Simulation:
Stage 1 ➔high-energy electrons in a crystal

metoda " multislice " : dividing a thick crystal into slices
"weak-phase-object aproximation"
Cowley and Moodie (1957)

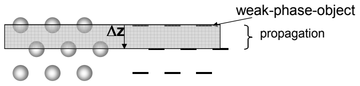

$$\Psi_{n+1}(\vec{r}) = \left[\Psi_n(\vec{r})q_{n+1}(\vec{r})\right] * p_{n+1}(\vec{r})$$

$$q_{n+1}(\vec{r}) = \exp\left[i\frac{\pi e}{\lambda E}\int_0^{\Delta z} V\ (x,y,z)dz\right]$$ Slice "transparency" function *(n+1)*

$$p_{n+1}(\vec{r}) = exp\left(-i\frac{k_z(x^2+y^2)}{2\Delta z}\right)$$ Propagator

HRTEM SIMULATION: STAGE II
➔ electrons in the optical system of the microscope

nonlinear image formation approximation
in partially coherent ilumination K. Ishizuk 1980

It takes into account the aberrations of the microscope optical system
➔
Contrast **T**ransfer **F**unction (CTF) , Contrast transfer function

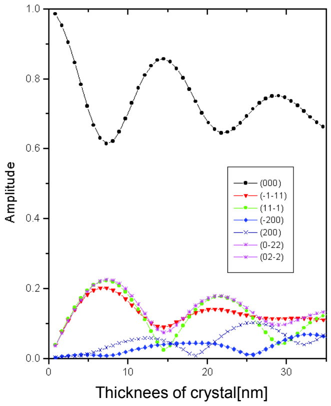

Primary beam amplitudes and the main beams are deflected (no absorption)

GaAs incident beam direction <110>

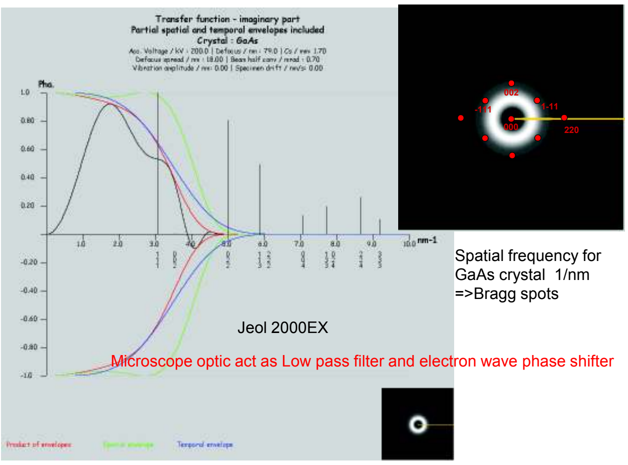

Jeol 2000EX

Microscope optic act as Low pass filter and electron wave phase shifter

Spatial frequency for GaAs crystal 1/nm
=>Bragg spots

Simulated HRTEMcontrast at 200 kV LaB_6

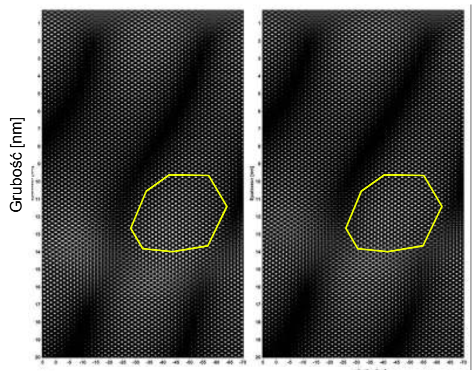

defocus [nm]

GaAs <110> Zone axis

$In_{0.5}Ga_{0.5}As$ <110> Zone axis

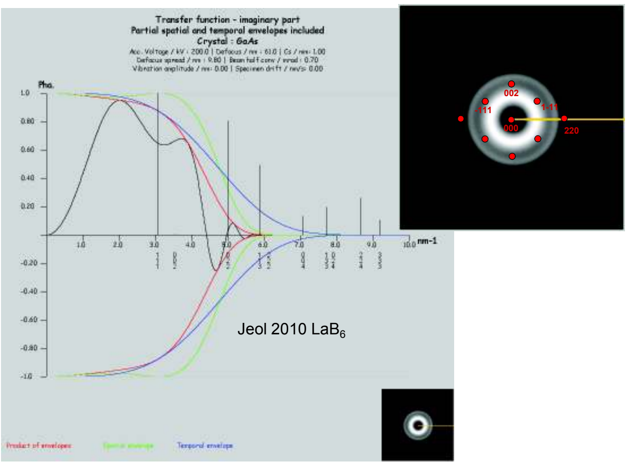

Jeol 2010 LaB_6

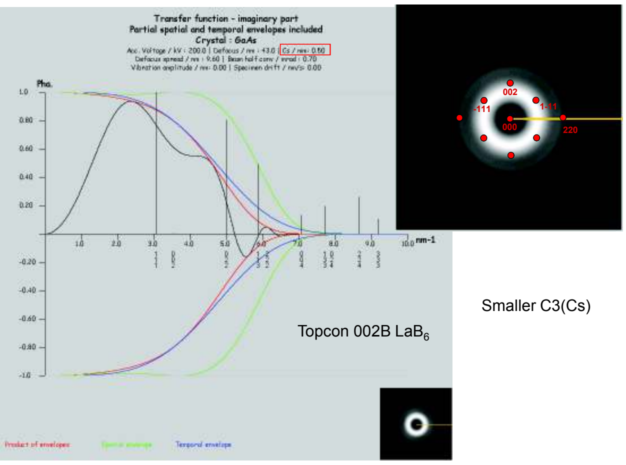

Topcon 002B LaB$_6$

Smaller C3(Cs)

Negative-spherical-aberration technique
- whit atoms
- Better contrast of light atoms

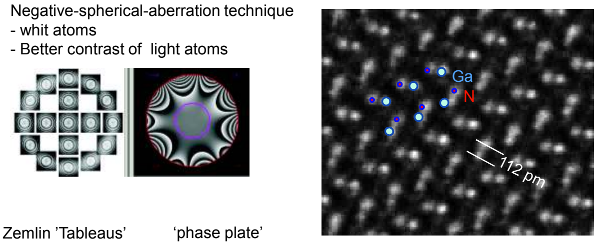

Zemlin 'Tableaus' 'phase plate'

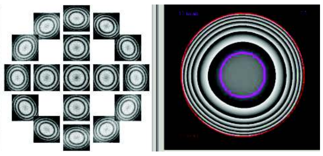

24 mrad beam tilt

50 YEARS OF

Electron Microscopy Group (EMG)
of Institute of Physics Polish Academy of Sciences

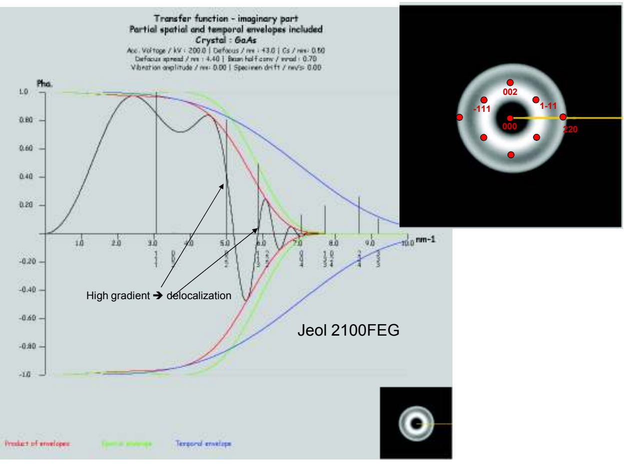

Jeol 2100FEG

Local strain measurement is a simple and popular method of QHRTEM

The main assumption :

The positions of the intensity maxima may correspond to the location of the atomic columns or tunnels between lattice sites or neither of them.
But this relation is constant in the whole analysed image .

Image simulations for axial HRTEM show that the measured lattice spacing depends locally on the imaging conditions (local foil misalignment and thickness variation) particularly for non-centrosymmetric structures/projection !!

Real word effect :
- surface relaxation
- artefacts due to sample preparation

Errors in processing:
- loss of information
- artifacts due to digitalisation, noise, filtering, interpolation

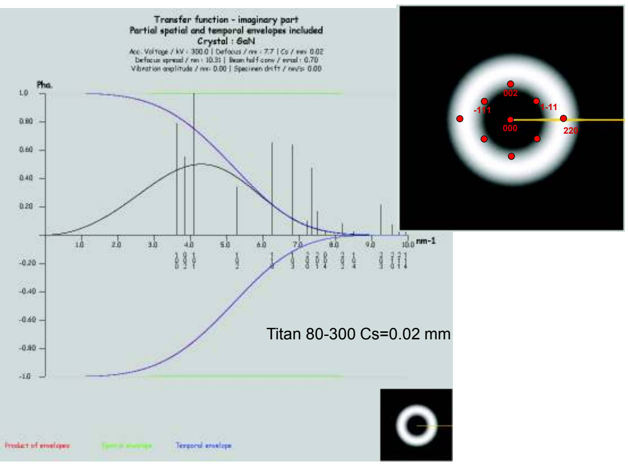

Titan 80-300 Cs=0.02 mm

Pseudomorphic growth, tetragonal distortion, biaxial stress

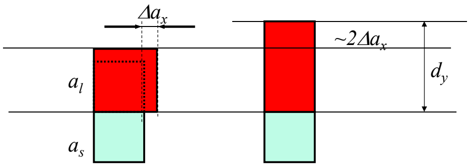

During pseudomorphic growth of a material with lattice parameter a_x *on a substrate with lattice parameter* a_s *the lattice parameter* $a_{x||}=a_s$.
However the lattice parameter in the y direction is $d_y > a_x$.

$$d_z = \alpha\Delta a_x + a_s$$

Dilatation of lattice in y is $d_y - a_s = \alpha\Delta a_x = \alpha(a_x - a_s)$ *where* $\alpha = \left(1 + 2\frac{c_{12}}{c_{11}}\right) = \frac{1+\nu}{1-\nu} \cong 2$

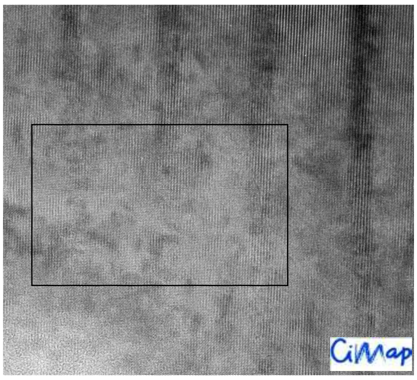

$In_{0.15}Ga_{0.8}N/GaN$

pseudomorphic

[$11\bar{2}0$] zone axis HRTEM image of InGaN (MBE) MQWs.

2D FE modeling

Geometry and border conditions similar as experimental

In function of the Indium concentration and t foil thickness

Homogeneous Indium distribution in QW

Chemical composition from Vegard`s Law

InGaN , GaN, InN, (ZnTe, CdTe)

$$a_{In_xGa_{1-x}N} = xa_{InN} + (1-x)a_{GaN}$$

$$a_x = xa_A + (1-x)a_B$$

$\varepsilon = (d_y - a_s)/a_s = \alpha(a_s - a_x)/a_s$

$\varepsilon = \alpha\Delta_{sx}/a_s \Rightarrow \Delta_{sx} = \varepsilon a_s/\alpha$

a_x - relaxed lattice parameter for composition x
$a_{A.}$ - relaxed lattice parameter for component A
a_B - relaxed latitce parameter for component B
a_s - relaxed lattice parameter for substrate
$a_B = a_s$
α – relaxation parameter

Local composition:

$$x(x,y) = \frac{a_s - a_x(x,y)}{a_A - a_S} = \frac{\Delta_{sx}}{\Delta_{AS}} = \frac{\boxed{\varepsilon(x,y)}a_s}{\alpha\Delta_{AS}}$$

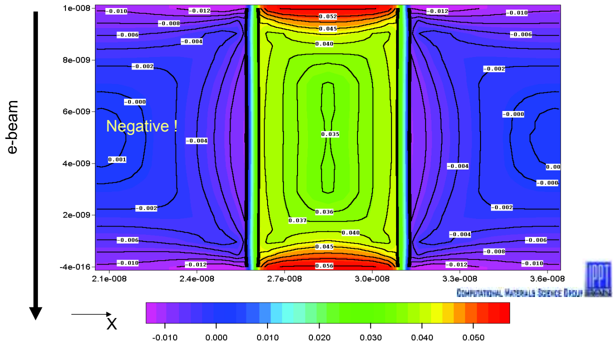

XY Cross-section of the TEM cross-section of MQW

Calculated distribution $\varepsilon_{xx}(x,y)$ after stress relaxation for In concentration %In=30 (QW/barriers geometry, in relation to GaN)

Thin foil effect

~Uniaxial stress ?

$$d_y = \alpha\Delta a + a_s$$

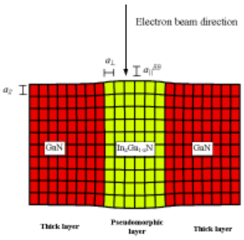

For (110) surface relaxation

$$\alpha = 1 + 4\frac{C_{44}C_{12}}{C_{11}^2 + 2C_{11}C_{44} + C_{11}C_{12} - C_{12}^2}$$

For CdTe/ZnTe

$\alpha_{ter} \approx 2.25$ $\alpha_{uniax} \approx 1.6$

40%

What is α ?

Biaxial or uniaxial ?

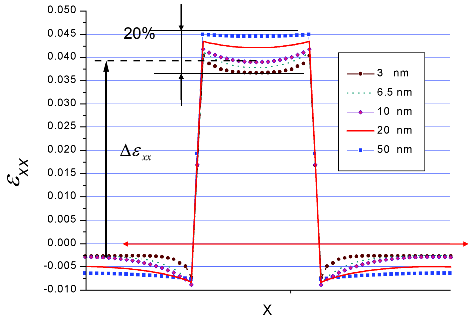

Profiles of $\varepsilon_{xx}(x)$ obtained by averaging $\varepsilon_{xx}(x,y)$ along the y direction for 30% indium concentration and t=5, 10, 15, 30 nm.

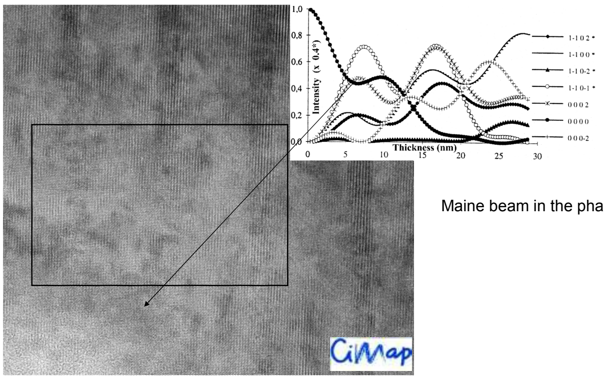

Maine beam in the phase

$[1 1 \bar{2} 0]$ zone axis HRTEM image of InGaN (MBE) MQWs .

Average profile
➔ better S/N ratio

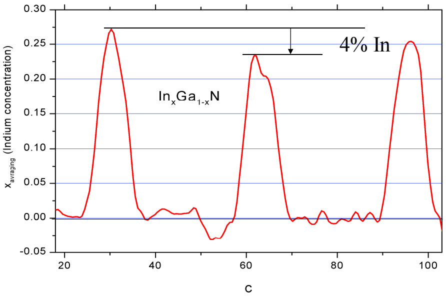

Thickness 5-10 nm

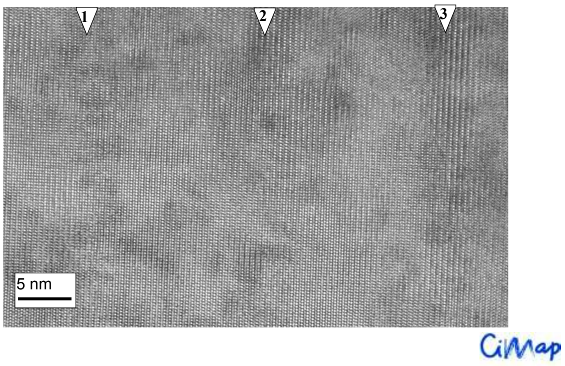

Averaging problem.

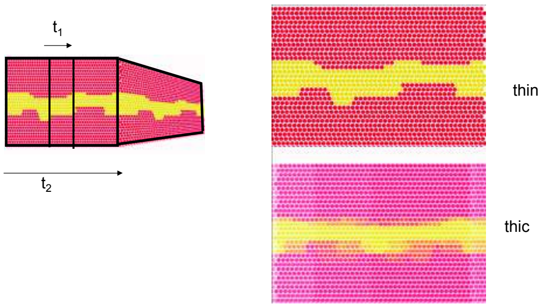

Thickness 5-10 nm

ε_{MAX}=0.030-0.038 ➔ A=720 ➔In_{Max}22-28%

Nominal ~15% A is determined from FEM modeling

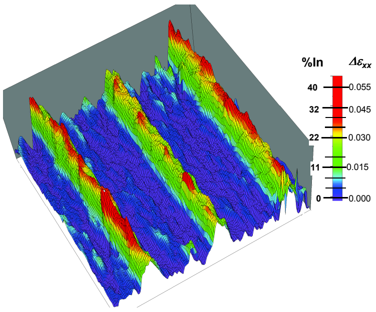

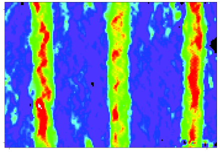

Surface plot of measured indium concentration; colour scales are common for $\Delta\varepsilon_{xx}$ and %In

---

Radiation demage False clusters

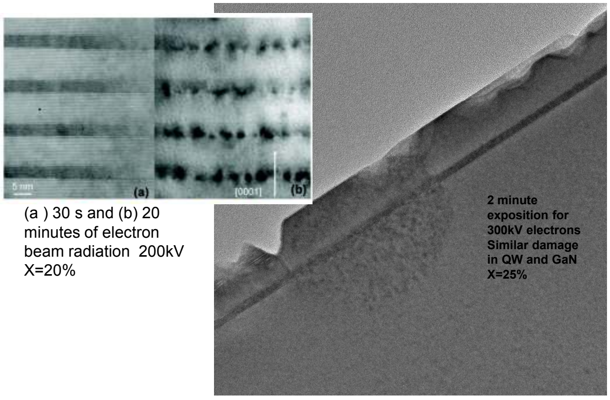

(a) 30 s and (b) 20 minutes of electron beam radiation 200kV X=20%

2 minute exposition for 300kV electrons Similar damage in QW and GaN X=25%

Electron energy loss spectroscopy and mapping the chemical composition

Electrons lose different amounts of energy depending on what they scattered

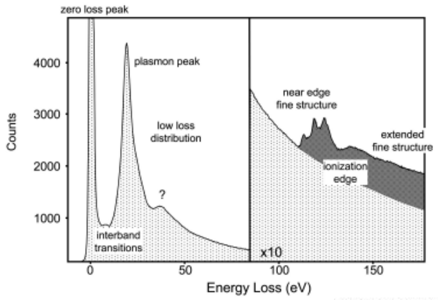

M. Kundmann: *Introduction to EELS in TEM*

Multiple linear least-squares fitting Mapping of Indium M_{45} Edge

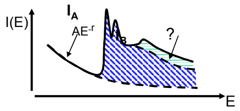

Ray D. Twesten

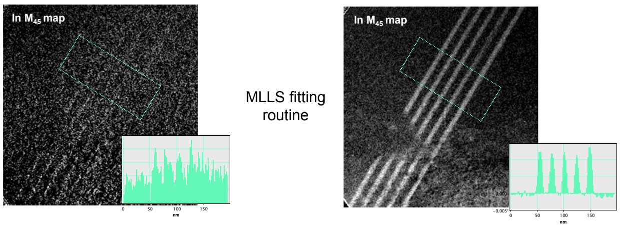

MLLS fitting routine

Such information can be obtained on a nanometric scale

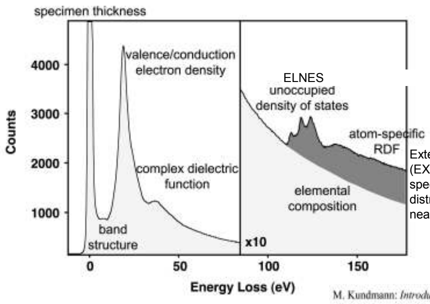

Extender fine structure (EXELFS) - atom-specific radial distribution of near neighbors (RDF)

M. Kundmann: *Introduction to EELS in TEM*

Z-contrast STEM

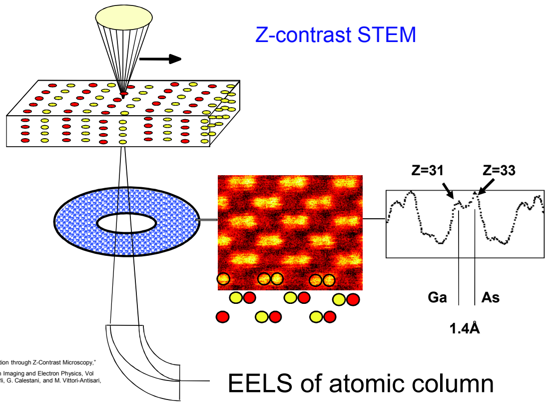

EELS of atomic column

Zródło:
S. J. Pennycook,
"Structure Determination through Z-Contrast Microscopy,"
p. 173 in Advances in Imaging and Electron Physics, Vol 123, ed. by P. G. Merli, G. Calestani, and M. Vittori-Antisari, 2002

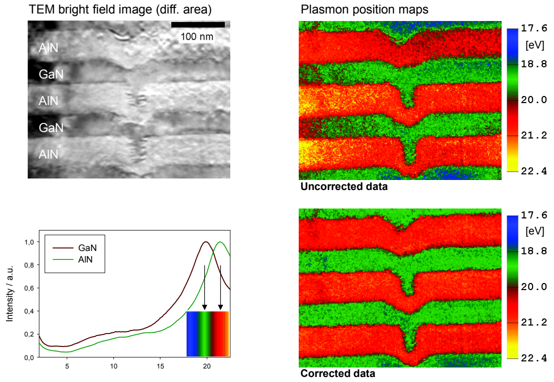

B. Schaffer, G. Kothleitner. W. Grogger published in Ultramicroscopy

---

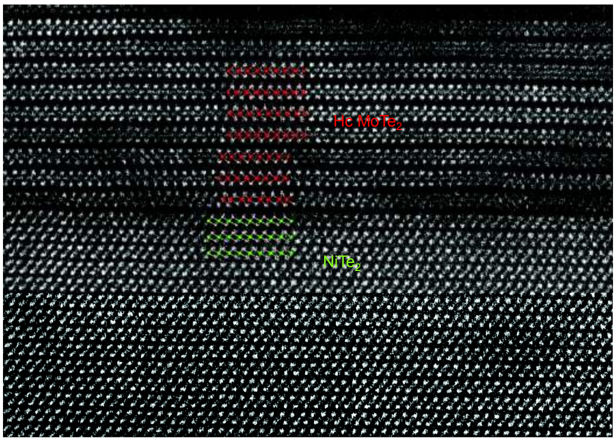

50 YEARS OF EMG STEM S.Kret IFPAN, MBE W.Pacuski WF-UW

Spectroscopic methods

Characteristic X-ray spectroscopy (EDX)

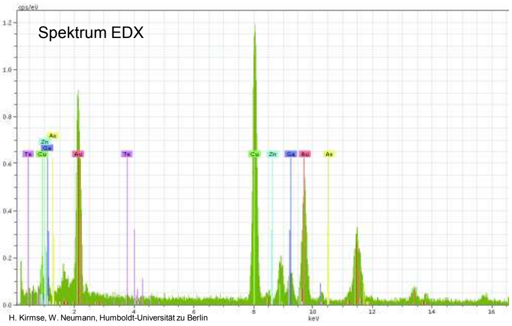

H. Kirmse, W. Neumann, Humboldt-Universität zu Berlin

Holografia elektronowa (niskiej rozdzielczości)

- ➔ precyzyjne pomiary zmiany fazy fali elektronowej
- ➔ wizualizacja lokalnych pól magnetycznych i elektrycznych,

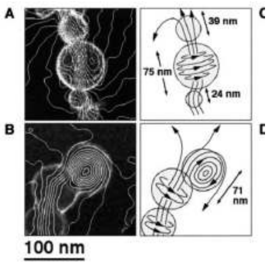

Nanocząski FeNi, wiry magnetyczne

RAFAL E. DUNIN-BORKOWSKI et. al. MICROSCOPY RESEARCH AND TECHNIQUE 64:390–402 (2004)

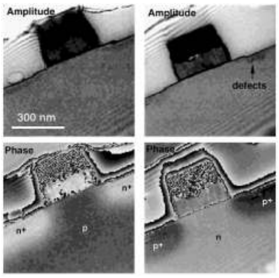

Tranzystory 0.3μm NMOS i PMOS
Amplituda i faza

W.D.Rau et. al, phys. Stat. Sol. (b) **222** , 213 (200)

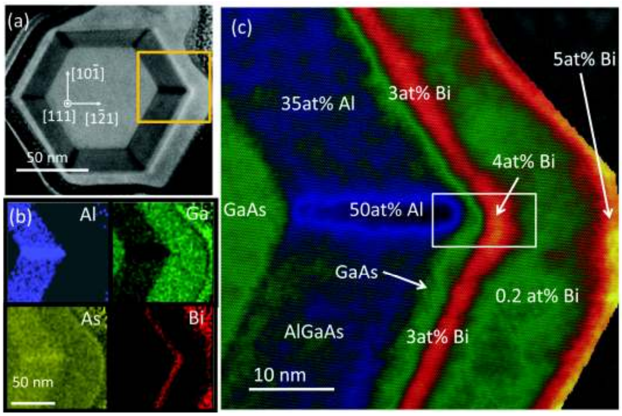

J. Sadowski, et. Al. et al. Bi incorporation and segregation in the MBE-grown GaAs-(Ga,Al)As-Ga(As,Bi) core–shell nanowires. Sci Rep 12, 6007 (2022)

ALLOYEAU *et al.* PHYSICAL REVIEW B **80**, 014114 (2009)

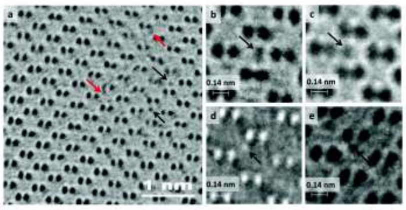

FIG. 1. (Color online) (a) Aberration-corrected images of a thin Ge crystal oriented along the [110] direction [black arrows show occupied interstitial sites, red arrows (dark gray) show column vibrations occurring during the acquisition time]. Magnified areas where an interstitial atom is observed, (b) and (c) In *T* sites, (d) In an *H* site that overlaps with a bond-centered site when the crystal is oriented along the [110] zone axis, (e) In an off-center site. Electron dose: 4.0×10^4 electrons/nm^2. Range of focus from −1 to −8 nm.

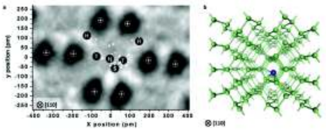

Phase Contrast
Single interstisal
Atom of Ge imaged and tracked !!

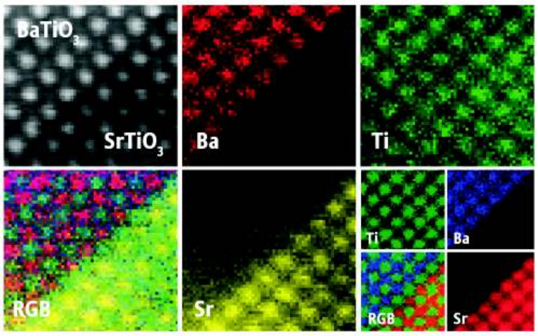

Atomic resolution STEM/EELS map on BaTiO$_3$/SrTiO$_3$ interface at 80 and 200 kV acceleration voltage.

Gatan Image filter Fei Titan 80KV

Projection problem

➔Tomogrphy

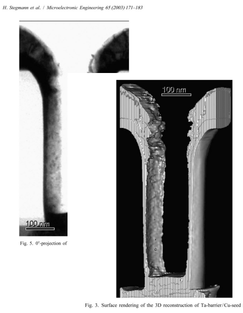

Fig. 5. 0°-projection of

Fig. 3. Surface rendering of the 3D reconstruction of Ta-barrier/Cu-seed sample 1.

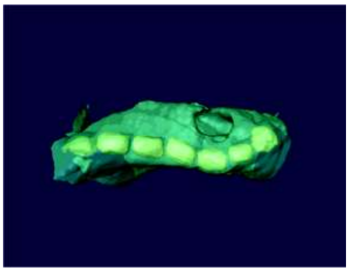

in-situ TEM

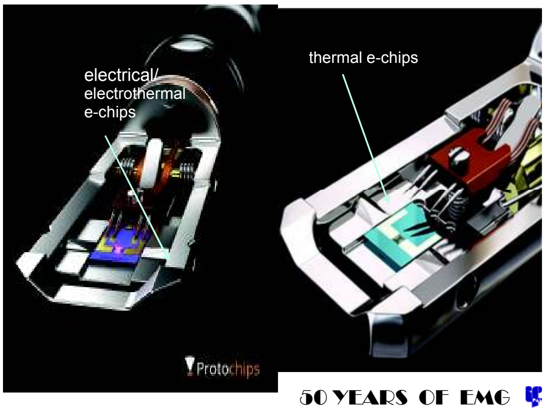

In-situ STEM observation – movable precipitates

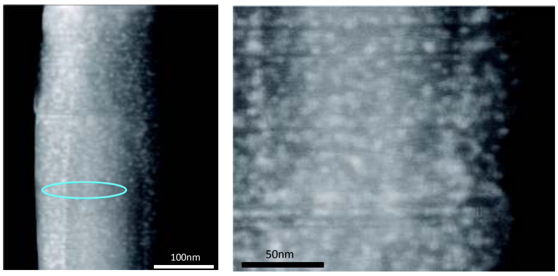

STEM and Image processing
A.Kaleta & S.Kret

---

thermal
e-chips

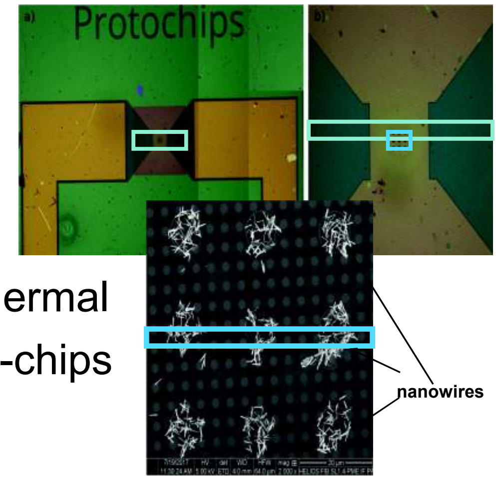

---

differential phase contrast, 4D STEM , and ptychography

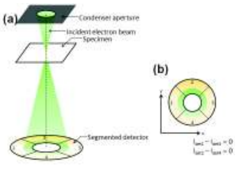

Central beam deflection
Due to magnetic /electric fields
Difference between segments
give signal for each pixel

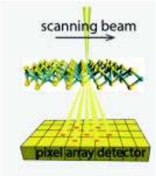

For every beam position
difraction pattern is captured
Separated disks

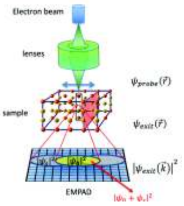

Overlapping disks !
Phase information can be
captured for spots
corresponding to spatial frequencies
beyond the limitations of the lens

In-situ izothermal annealing

In-situ
experiment:
T = 500°C
Annealing time:
30 min

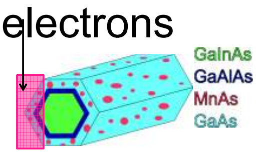

STEP I
Projected distortion of bent
elastically strained Core Shell ZnTe/CdZnTe NW

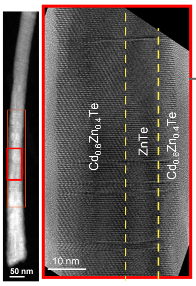

HRTEM [110] zone axis

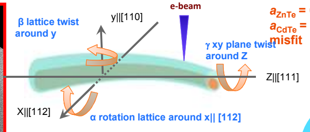

Lattice constant:
a_{ZnTe} = 6.103Å
a_{CdTe} = 6.483Å ~6% of misfit

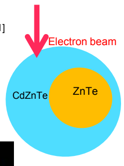

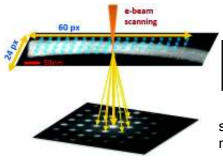

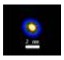

Probe size

scanning electron
nano beam diffraction

Latice distortion mapping using electron nano-beam diffractior

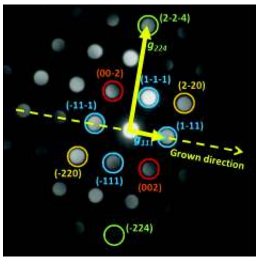

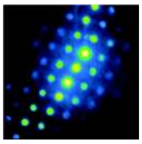

Experimental 1440
STEM-CBED patterns
Convergence angle ~1 mrad
ULTRASCAN 1000 CCD

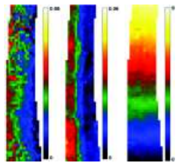

Strain in axial (grown) direction - ε_{zz}

Strain in radial direction - ε_{xx}

In-plane bending Rotation of DP

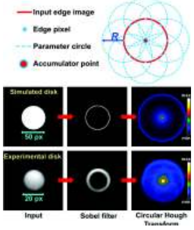

Experimental nano- diffraction pattern [110] ZA

Inhomogeneous intensity distribution in disks

Contain useful information => no precesion !

Sobel Filter + Circular Hough transform (CHT) with variable radius solves the problem of the variation of the disk radius

GMS skrypt

S. Kryvyi, S. Kret and P. Wojnar, Nanotechnology, 33(19), 195704, (2022)

FEM modeling of core-shell hetero-nanowires

Solid Mechanics

Linear Elastic

Initial Stress and Strain

Anisotropic elastic material

ZnTe:

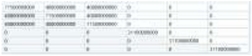

CdTe:

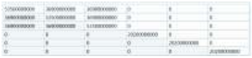

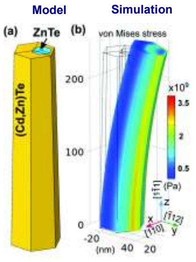

Initial model

Zone axis and off-axis diffraction

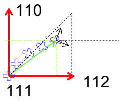

α rotation of xy plane around x|| [112] ?

γ xy plane twist around Z || [111] ?

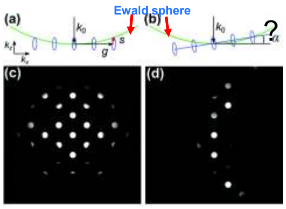

Zone axis diffraction pattern

Off-axis diffraction pattern

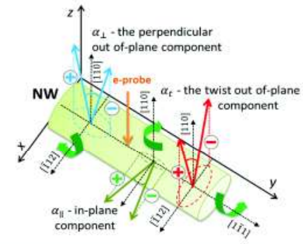

The scheme represents definition of misorientation angles. $\alpha_{\parallel}$ – angle denote in-plane component of lattice bending and $\alpha_{\perp}$, α_{τ} – out of-plane components. The sign "+" and "-" represents direction of bend.

STEP III
iterative Fitting of FEM and experimental maps

We have:

- **Asymmetrical core-shell configuration**
- **Core -> ZnTe**
- **Shell -> $Cd_xZn_{1-x}Te$**
- **Radius of the NW**

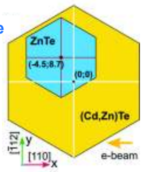

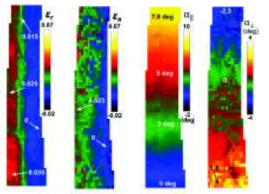

Strain in radial direction

Strain in axial (growth) direction

In-plane bending

Out-of-plane bending

We still need:

- **Cd content in the shell?**
- **Core radius?**
- **Core position in the NW (x,y)?**

- **And we make same additional assumption …………….**

STEP II Determination α, β local misorientation, and local thickness

Preparation of a series simulated patterns for various α, β misorientation and thickness (Bloch wave or multislice simulation)

For each beam position comparison of experimental diffraction with simulated patterns

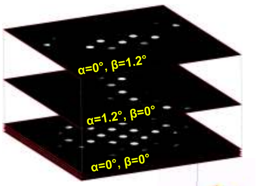

Results:

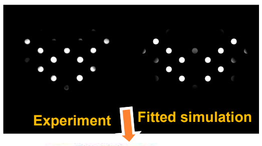

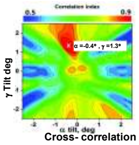

Cross- correlation Map

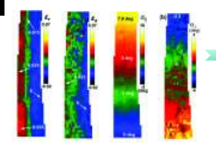

Strain in radial direction

Strain in axial direction

In-plane bendin

Out-of-plane bending

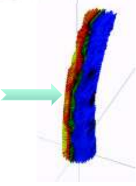

reconstructed thickness
color mapping => ε_{xx}

Cross-section of best fit simulated core-shell NW

QUASI/pseudo-Tomography from one projection -> limited radiation damage , the same object structure

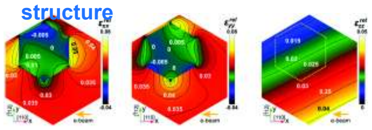

$$\varepsilon^{rel}_{ZnTe} = \frac{d^{core}_{ZnTe} - d^{teor}_{ZnTe}}{d^{teor}_{ZnTe}}$$

$$\varepsilon^{rel}_{CdZnTe} = \frac{d^{shell}_{CdZnTe} - d^{teor}_{ZnTe}}{d^{teor}_{ZnTe}}$$

maps of relative strain calculated using relaxed ZnTe as a reference

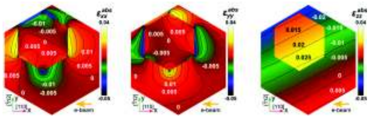

Absolute strain calculated in terms of relaxed ZnTe core and $Cd_{0.57}Zn_{0.43}Te$ shell values

S. Kryvyi, S. Kret and P. Wojnar, Preprint in *arXiv*, https://doi.org/10.48550/arXiv.2301.05527

Magentic Skyrmions in FeGe after field cooling to 94

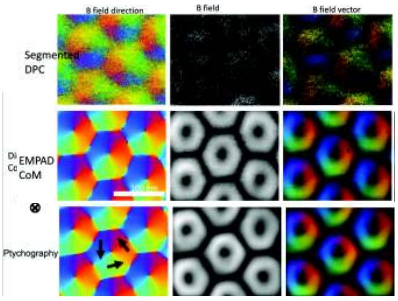

D. McGrouther *et al*, *New J. Phys.* **18**, 095004 (2016)

Some week points of TEM

- ➔ Necessity to perform the preparation
- ➔ Destruction of the material
- ➔ Poor sampling local information only from electron-transparent regions but up to 0.1-0.5 mm2 for the best samples preparation protocols
- ➔ Preparation artifacts
- ➔stress relaxation in a thin foil
- ➔amorphization, radiation defects by Ions during preparation
- ➔radiation damage with electrons during observation

- ➔ the sample is no longer representative due to
- ➔ jonization and destruction of chemical bonds heating and diffusion of components in poorly conducting samples, knocout or shifting atoms, spraying

- ➔ high costs of equipment,
- ➔ time-consuming preparation of thin cross-sections
- ➔ complicated "keyboardology" and data interpretation

- ➔ imagination and knowledge of a microscopist (still needed)

Ultimate lateral resolution – better than the thermal vibration of atoms with a perovskite – PrScO3 - structure. Multi-Slice ptychography for thic sample

New record of resolution **22pm David A. Muller groupe at** Cornell University

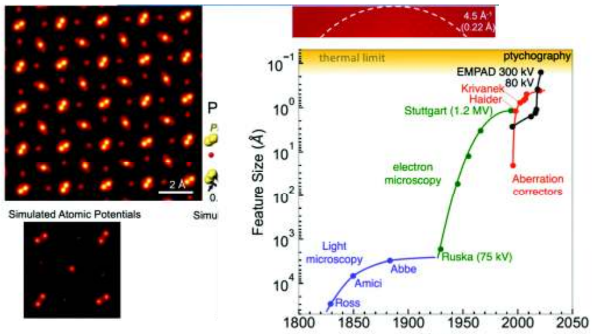

Z. Chen et al. Science 2021 , 372, p. 826

TEM methods are the most powerful fast progressing characterization tools for crystalline nanomaterials with few limitations